



SPECIAL TOPIC: High-performance Structural Materials

Effects of twin thicknesses on incoherent twin-boundary structures in face-centered cubic metals

Zhanxin Wang¹, Yizhong Guo¹, Yan Ma¹, Chengpeng Yang¹, Yadi Zhai^{1*}, Xin Yan^{2*}, Lihua Wang^{1*} and Xiaodong Han¹

Twin-structured materials have garnered significant attention owing to their exceptional mechanical properties [1,2], such as ultrahigh strength [3–5] and improved fatigue resistance [6–8]. These mechanical properties are directly influenced by their atomic-scale structures. Consequently, numerous studies have investigated the atomic structures of twin boundaries (TBs) in face-centered cubic (FCC) metals. Among TBs, the coherent TB (CTB) is a special grain boundary (GB) with perfect symmetry and coherent structure, and its deformation mechanism varies with the twin thickness [9–17]. Similar to CTBs, incoherent TBs (ITBs) are also important GBs that significantly impact the mechanical properties of materials. In recent decades, extensive research has been conducted to explore the atomic-scale structures of ITBs, leading to the proposal of various models [18–22]. Theoretical models have suggested that ITBs consist of a series of Shockley partial dislocations with Burgers vectors of $1/6\langle 112 \rangle$, without any displacement along the $\langle 111 \rangle$ direction [20–22]. This has led to the widespread belief that lattice displacement along the $\langle 111 \rangle$ direction (perpendicular to the CTB) between the two sides of the ITB interface should be disregarded. However, experimental observations and molecular dynamics simulations have revealed evident lattice displacement along the $\langle 111 \rangle$ direction between the two sides of the ITB interface [23], seemingly contradicting the theoretical predictions. This discrepancy between the theoretical model and the experimental findings requires further systematic investigation. Furthermore, previous studies [24–26] have revealed that the GB plane and angle can significantly affect the GB structure. Both experimental and simulation results [27–32] have demonstrated that GB transitions can occur in various material systems due to heating and impurity concentrations. However, whether changes in size alone can lead to ITB transitions remains unknown.

In this study, we conducted molecular statics (MS) simulations to investigate the influence of twin thicknesses on the atomic structures of ITBs in four FCC metals: Ag, Cu, Ni, and Al. When ITBs were thin, the lattices on both sides were located approximately on the same horizontal plane, exhibiting no significant displacement along the [111] direction. However, as the ITB thickness increased, the displacement along the [111] direction between the ITB interfaces increased, approaching a nearly constant value when the thickness exceeded approximately 80 atomic layers. We observed that the CTB and matrix

lattice had a confinement effect that suppressed the displacement along the [111] direction of the ITB. This confinement effect decreased with increasing distance from the CTB, leading to the observed size effect on lattice displacement along the [111] direction. Additionally, the displacements along the [111] direction of the ITBs exhibited a negative linear relationship with the stacking fault energy (SFE) in the thick twins.

To examine these effects, we constructed atomic models of Ag, Cu, Ni, and Al with twin structures of different ITB thicknesses. A typical example is shown in Fig. 1a. In these models, the atoms of the FCC crystal structure, hexagonal close-packed (HCP) crystal structure, and others are depicted in green, red, and white, respectively. The X, Y, and Z axes align with the $[110]$, $[11\bar{2}]$, and [111] directions, respectively. A periodic boundary condition was applied in the X direction while maintaining the surfaces in the Y and Z directions free. Fig. 1b shows the two-dimensional (2D) structure projected along the $[110]$ direction. The figures clearly show that the ITB (white atoms) is parallel to the [111] direction, and the CTBs (red atoms) are perpendicular to that direction. The atomic interactions were described using embedded atom method (EAM) potentials [33], and the energy of the structures was minimized using a conjugate gradient (CG) approach to obtain stable structures. In this simulation, the corresponding atomic displacement was defined as the difference between the atomic spacing in the twin-structured models and that in a perfect FCC structure (see the calculation methods and Fig. S1 in the Supplementary information for details). The displacements of each atom along the [111] and $[11\bar{2}]$ directions were measured, and the atomic models were created using ATOMSK (see the detailed modeling method and Fig. S2 in the Supplementary information) [34]. The simulations were conducted using a large-scale atomic/molecular massively parallel simulator (LAMMPS) [35] and the configurations were rendered in OVITO [36].

The displacement maps (along the [111] direction) of Cu models are presented in Fig. 2a–d, where the color variations from dark blue to red indicate displacements ranging from -0.25 to 0.5 Å. Notably, the displacement along the [111] direction exhibited a clear twin-thickness effect. Fig. 2a shows that the ITB had a thickness of nine atomic layers, and the lattices on both sides of the ITB resided on nearly the same

¹ Beijing Key Laboratory of Microstructure and Properties of Advanced Materials, Beijing University of Technology, Beijing 100124, China

² School of Mechanical Engineering and Automation, Beihang University, Beijing 100191, China

* Corresponding authors (emails: wlh@bjut.edu.cn (Wang L); yan_xin@buaa.edu.cn (Yan X); ydzhai@bjut.edu.cn (Zhai Y))

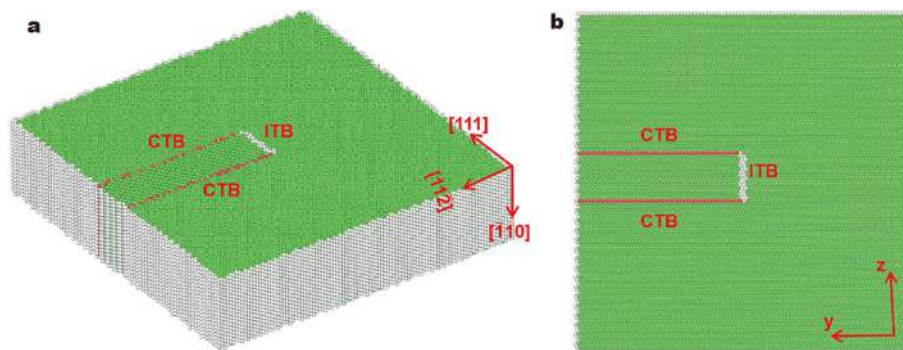


Figure 1 (a) 3D structure of the model and (b) 2D view projected along the $[1\bar{1}0]$ direction (atom colors denote crystal structures according to common neighborhood analysis, where red, green, and white indicate HCP, FCC, and others, respectively).

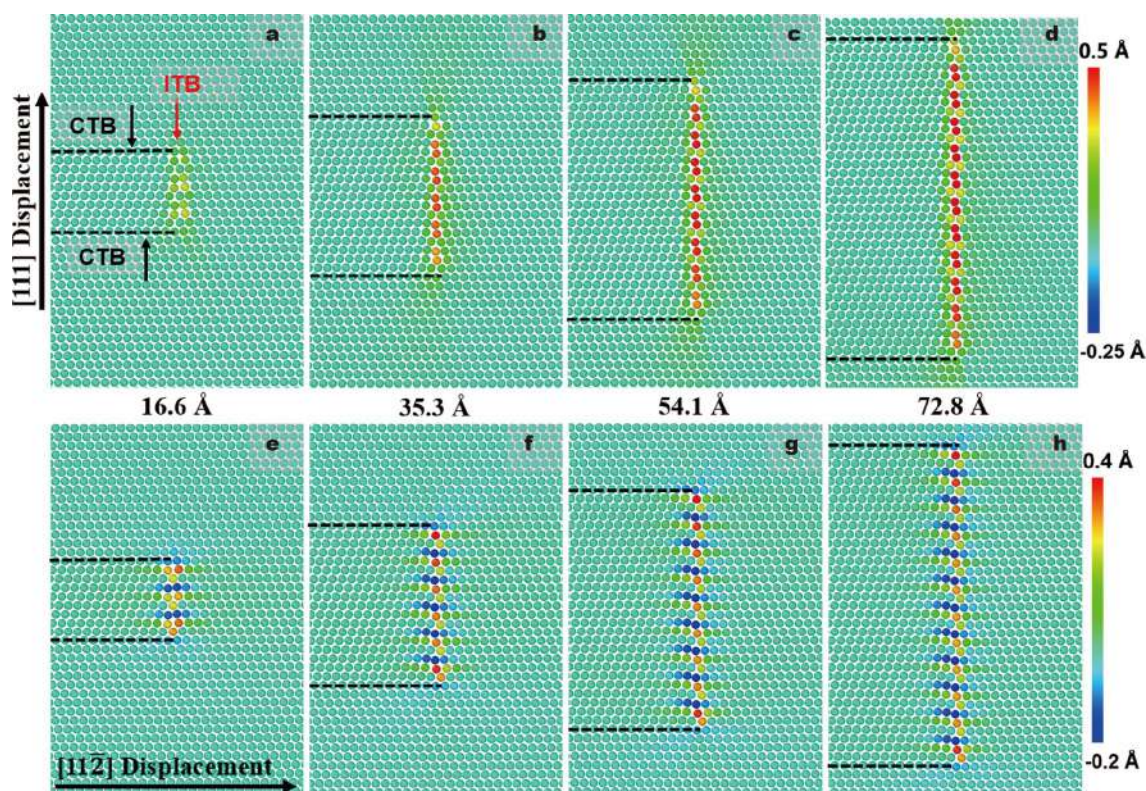


Figure 2 2D views and displacement maps of Cu with twin thicknesses of $n = 9, 18, 27, 36$ atomic layers: (a–d) displacement maps along the $[111]$ direction; (e–h) displacement maps along the $[11\bar{2}]$ direction.

horizontal plane. The interface appeared light green, indicating minimal displacement along the $[111]$ direction. However, for twins with greater thickness, as shown in Fig. 2d, significant displacements occurred along the $[111]$ direction. Interestingly, as the twin thickness increased, the overall color of the ITB changed from light green to dark red, indicating an increase in displacement along the $[111]$ direction (Fig. 2a–d). This serves as direct evidence that the ITB structure is subject to a strong size effect. We further investigated the lattice displacements along the $[111]$ direction of the ITBs in Al, Ni, and Ag and observed the same behavior (Figs S3–S5). Additionally, we used other EAM potentials to verify the effect of the potential on this size effect and similar size effects on the ITB were observed (Fig. S6). Moreover, considering the effect of kinetic energy, this size effect was also observed using molecular dynamics simulations

(Fig. S7). Furthermore, our experimental observation on twin-structured Pt also exhibited this size effect on the ITB structure (Fig. S8), indicating its universality.

Maps of the relative displacement along the $[11\bar{2}]$ direction are shown in Fig. 2e–h. The color variations from dark blue to red indicate displacements between -0.2 and 0.4 Å. A clear periodicity can be observed, with atoms at the ITB interface exhibiting a repeatable order of dark blue, orange, and green, which remained consistent regardless of twin thickness. Correspondingly, the strain at the ITB interface also exhibited periodicity, with a repeatable order of compressive, tensional, and nearly zero strains. This structure aligns with previous studies where the ITB consisted of periodic sets of partial dislocations b2, b1, and b3 [21,37,38]. Here, “b1” represents an edge partial dislocation with a Burgers vector of $1/6[11\bar{2}]$, whereas “b2” and “b3”

are mixed types with Burgers vectors of $1/6[211]$ and $1/6[1\bar{2}1]$. Our atomistic simulations confirmed that the ITBs of Cu, Al, Ni, and Ag contained the same periodic sets of partial dislocations b_2 , b_1 , and b_3 .

Based on the MS simulations, the statistical results of the lattice displacements along the $[111]$ and $[11\bar{2}]$ directions of the ITBs in Cu, Al, Ni, and Ag are presented in Fig. 3. The X-axis represents the index of the atomic layers from the topmost TB (where the middle TB is defined as the zero-atomic layer) to the bottommost TB. The Y-axis, as shown in Fig. 3a–d and e–h, represents the lattice displacement along the $[111]$ and $[11\bar{2}]$ directions, respectively. Each subgraph includes the statistics of the ITBs with thicknesses of 9, 18, 27, and 36 atomic layers. Fig. 3a shows the statistics for displacement along the $[111]$ direction in Cu. The overall shapes of the dotted lines resemble arches, with higher values in the middle and lower values at the two ends. The red dotted line denotes the displacement of each layer of the ITB with a thickness of nine atomic layers. Here, the arch shape is not obvious, and the displacements of every three layers are small. However, in relatively thicker twins, as indicated by the orange, green, and blue dotted lines, clear arches can be seen. Additionally, as the twin thickness increased, the top of the arch also increased correspondingly, following the same regularity as the color changes in Fig. 2a–d. This suggests that the displacement along the $[111]$ direction increased with twin thickness, with the maximum displacement occurring near

the middle of the ITBs. Similar results were observed for other FCC metals (Al, Ni, and Ag), as shown in Fig. 3b–d, indicating the universal nature of this size effect in FCC metals. Fig. 3e shows the statistics for displacement along the $[11\bar{2}]$ direction in Cu. The displacement along the $[11\bar{2}]$ direction exhibited periodicity with repeatable values of ~ -0.57 , 0.82 , and 0.14 Å every three atomic layers. Similar periodic features were observed for other FCC metals (Al, Ni, and Ag) along the $[11\bar{2}]$ direction, as shown in Fig. 3f–h.

To explore the effects of twin thickness on the $[111]$ displacement and validate its size effect, we plotted the normalized maximum displacement (the ratio of the maximum displacement to the lattice constant) along the $[111]$ direction against the variations in twin thickness in Ag, Cu, Ni, and Al (Fig. 4a). The results show that the normalized maximum displacement increased with increasing twin thickness. Particularly, the increase in the normalized maximum displacement was more pronounced when the twin thickness was less than ~ 60 layers. However, for twin thicknesses exceeding 80 layers, the normalized $[111]$ displacement appeared to approach a constant, with a less noticeable increase as the twin thickness continued to increase. Consequently, the validation of the twin-thickness effect was ~ 80 layers. Notably, this trend was valid for Al, Ni, Cu, and Ag, indicating a general phenomenon. The vertical dashed line in Fig. 4a indicates that the magnitudes of the normalized $[111]$ displacements of the 108-layered ITBs for the four FCC

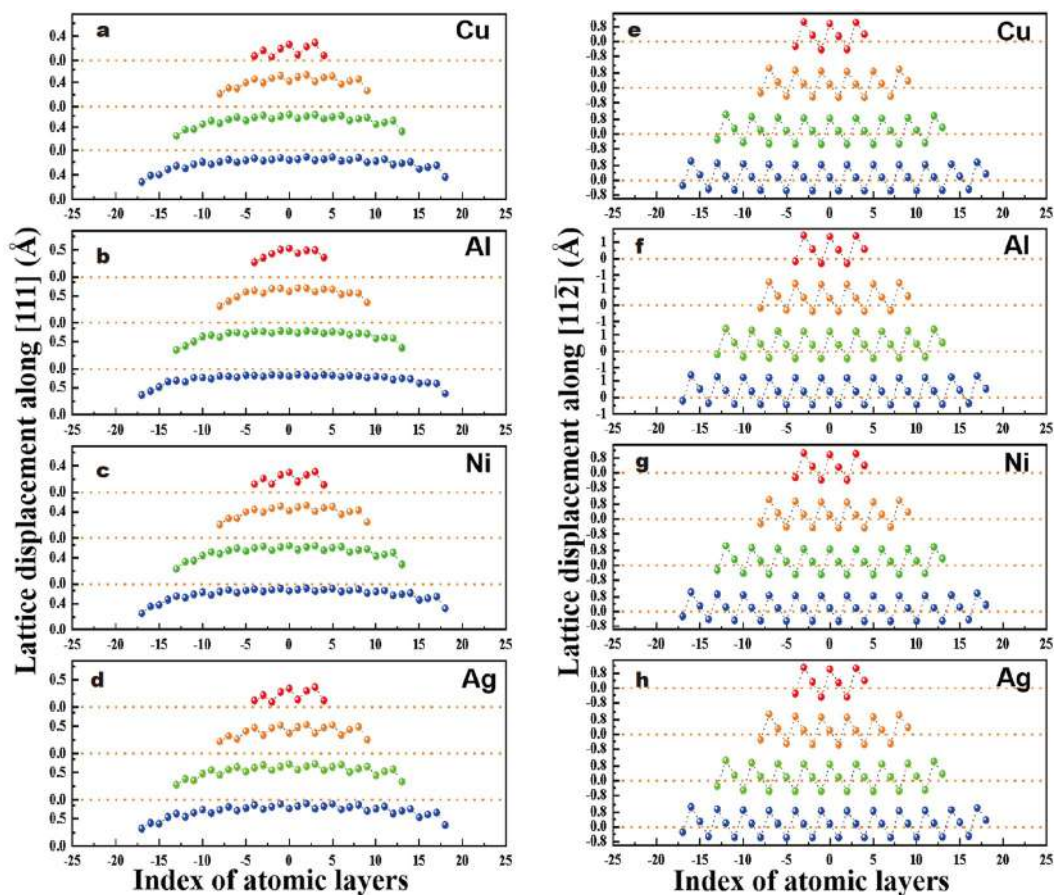


Figure 3 Statistical results of the measured lattice displacements: (a–d) lattice displacements along the $[111]$ direction at the ITBs for Cu, Al, Ni, and Ag, respectively; (e–h) lattice displacements along the $[11\bar{2}]$ direction at the ITBs for Cu, Al, Ni, and Ag, respectively.

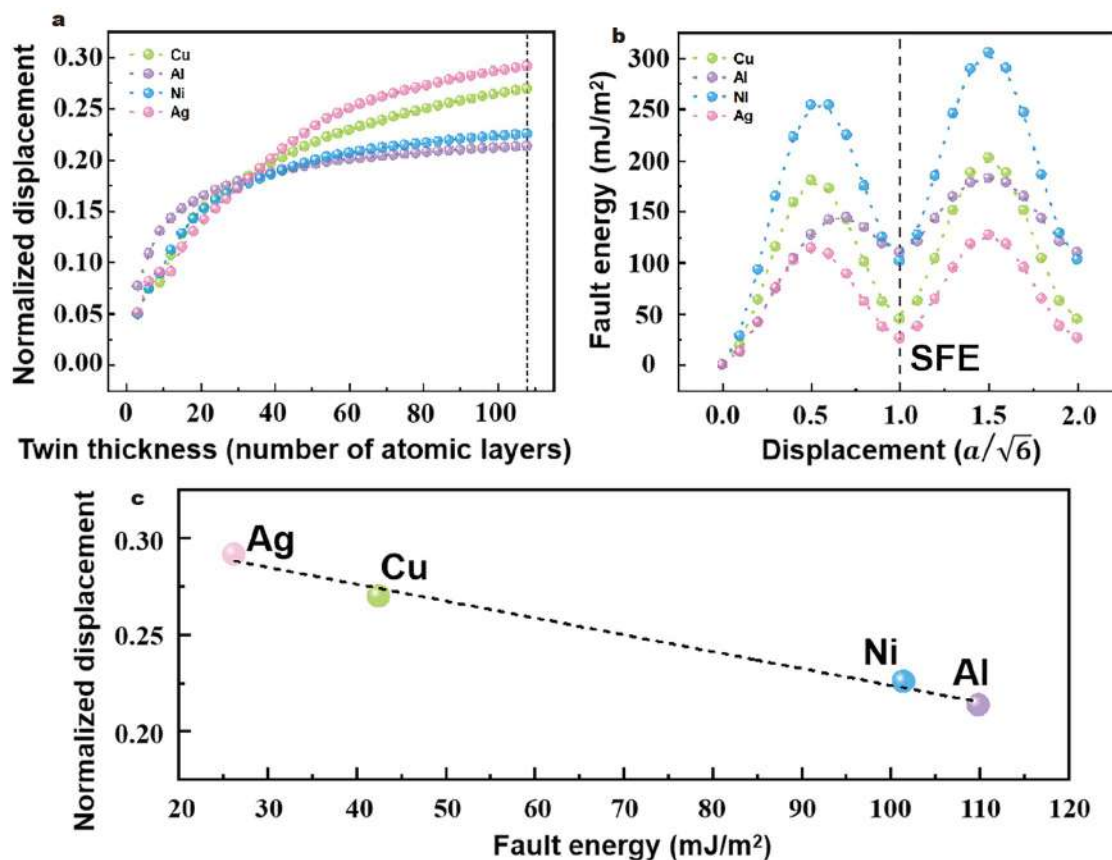


Figure 4 (a) Normalized maximum [111]-direction displacements vs. twin thickness. (b) SFE curves of Ag, Cu, Ni, and Al. (c) Fitted line showing the relationship between the normalized maximum [111]-direction displacements of the 108-layered ITBs and SFE.

metals followed the order $\text{Ag} > \text{Cu} > \text{Ni} > \text{Al}$. Furthermore, based on our calculations, we found that the SFE significantly influenced the normalized [111] displacements. Fig. 4b shows the calculated fault-energy curves of Ag, Cu, Ni, and Al, where the magnitude of the SFE followed the order $\text{Ag} < \text{Cu} < \text{Ni} < \text{Al}$ (indicated by the black vertical dashed line). Using the information from Fig. 4a, b, we generated a plot of the normalized maximum displacement against the SFE (Fig. 4c). The normalized displacement values along the [111] direction exhibited a negative linear relationship with the SFE in thick twins. In other words, as the SFE increased, the normalized values decreased. The corresponding fitted equation was given by

$$d/a \approx 0.31 - k_0 \times \gamma_{\text{sf}} \quad (1)$$

where d is the displacement along the [111] direction, a is the crystal constant, k_0 is a constant coefficient for FCC metals (with a unit of $10^{-4} \text{ m}^2 \text{ mJ}^{-1}$), and γ_{sf} is the value of the SFE.

Previous atomistic simulations have shown that the displacement along the [111] direction arises from ITB dissociation. The ITB can spontaneously dissociate, forming the 9R phase [37,38]. This 9R phase tilts away from the FCC phase at an angle of approximately 13.28° , leading to displacement along the [111] direction. The normalized displacement increases with the dissociation distance, which scales inversely with the SFE [37]. Consequently, the displacement along the [111] direction exhibits a negative linear relationship with the SFE of the metals. The displacement maps shown in Fig. 5 reveal that the dissociation distance of the ITB decreases with increasing SFE, with the ITB dissociation distance of the four FCC metals following the order

$\text{Ag} > \text{Cu} > \text{Ni} > \text{Al}$. For Ag, the ITB structure exhibits a relatively distinct 9R structure, as evidenced by the specific 9R structure analysis shown in Fig. S9.

Here, the CTB can have a confinement effect on the displacement along the [111] direction of the ITB, arising from various factors. The strain field and displacement generated by the 9R phase along the [111] direction disrupt the equilibrium and stable state of the CTB and matrix. Consequently, the CTB and matrix restrict the displacement along the [111] direction. Moreover, the lattice orientation in the matrix differs from that of the twin, causing the 9R-phase-generated field/displacement along the [111] direction to undergo disturbance and release upon penetrating the matrix. Moreover, this confinement effect decreases with increasing distance from the CTB. For thinner ITBs, the effect is sufficient to suppress the displacement along the [111] direction of the ITB. Thus, our study showed that practically no lattice displacement occurred along the [111] direction between the ITB interfaces, as shown in Fig. 2a. However, in thicker ITBs, the confinement effect becomes insufficient to suppress the [111]-direction displacement of the entire ITB. Thus, an obvious displacement along the [111] direction was observed. The lattice displacement along the [111] direction increases as the distance from the CTB increases, with the maximum displacement constantly occurring in the middle of the ITBs. To further verify this, we compared the lattice displacements along the [111] direction of ITBs with and without CTBs. Fig. 5a shows the ITB models of Ag, with two CTBs and no CTBs in the left and right models, respectively. The

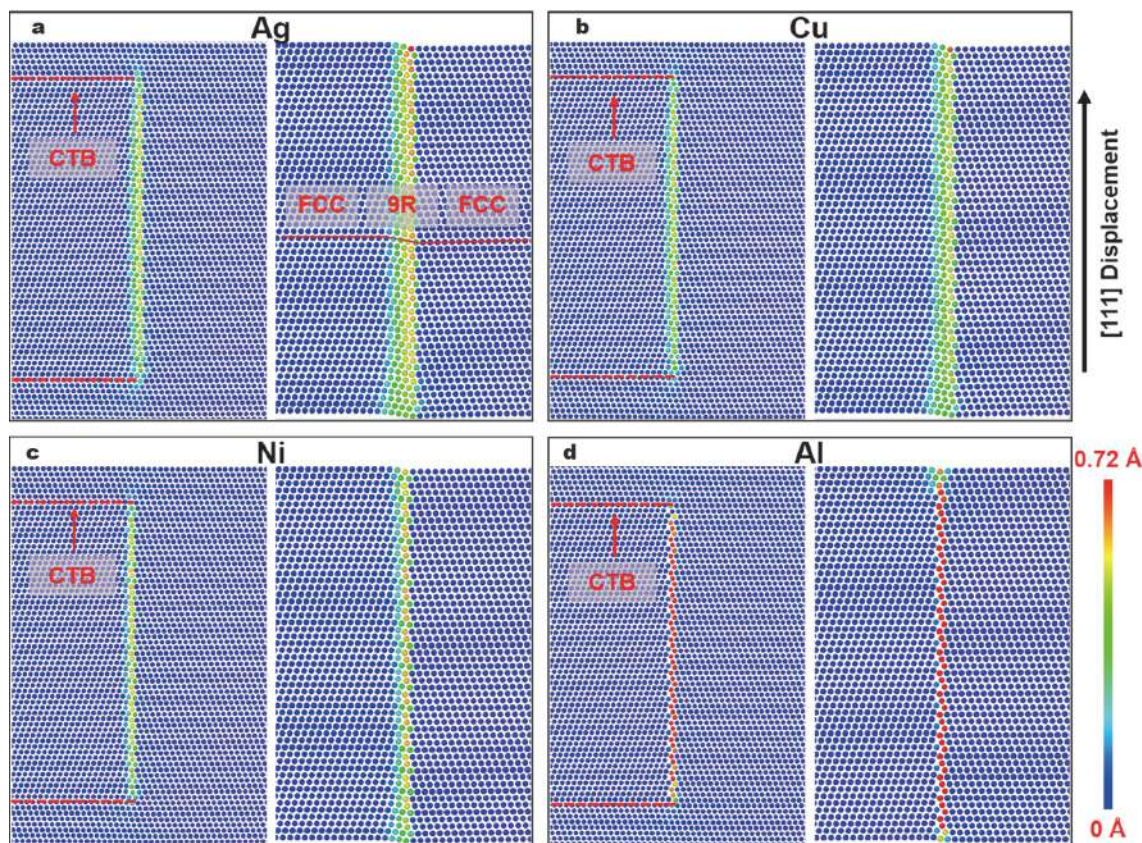


Figure 5 (a–d) Structures and [111] displacement maps of the 54-layered ITBs with (left) and without (right) CTBs for Ag, Cu, Ni, and Al, respectively.

figure shows that the color of the ITB without CTBs is more intense than that of the ITB with CTBs, indicating that the [111]-direction lattice displacement of the former is greater than that of the latter. This proves that the CTBs have a confinement effect on the [111] displacement. Fig. 5b–d show that the other metals (Cu, Ni, and Al) exhibit similar behaviors, indicating that the confinement effect of the CTBs is universal. Moreover, the structure of the GB can significantly affect the mechanical properties of metals [39,40]. Our results, which revealed a strong size effect in the ITB structure, offered a potential explanation for the variation in mechanical properties observed in twin-structured metals with different twin thicknesses. Moreover, although theoretical models suggesting no lattice displacement along the [111] direction between the two sides of the ITB interface [20–22], our experimental observations and molecular dynamics simulations show conflicting results. Our findings demonstrated that both the size and SFE can affect the lattice displacement along the $\langle 111 \rangle$ direction, offering valuable insights to resolve this puzzle. Previous studies have primarily focused on the twin thickness effect on dislocation behavior, overlooking its impact on the atomic-scale structure of ITBs. This effect represents another critical factor influencing the mechanical properties of twin-structured metals [41].

In summary, we statistically analyzed the structures of ITBs with different thicknesses of Ag, Cu, Ni, and Al and observed a significant size effect in the displacements along the [111] direction of the ITBs in these metals. Thinner ITBs exhibited a confinement effect by the CTBs, effectively suppressing displacement in the [111] direction. However, as the twin thickness increased, the confinement of the CTB was no longer sufficient

to suppress the displacement along the [111] direction, resulting in an obvious size effect on the ITB structure. Furthermore, we found that the normalized [111] displacements of the ITBs exhibited a negative linear relationship with the SFE in FCC metals. Our findings provide valuable insights into understanding the distinct mechanical properties of twin-structured metals with different thicknesses.

Received 18 May 2023; accepted 8 August 2023;
published online 27 September 2023

- Lu K. Stabilizing nanostructures in metals using grain and twin boundary architectures. *Nat Rev Mater*, 2016, 1: 16019
- Ke X, Ye J, Pan Z, *et al.* Ideal maximum strengths and defect-induced softening in nanocrystalline-nanotwinned metals. *Nat Mater*, 2019, 18: 1207–1214
- Lu L, Chen X, Huang X, *et al.* Revealing the maximum strength in nanotwinned copper. *Science*, 2009, 323: 607–610
- Zhu Y. Catch twin nucleation in action at atomic scale. *Sci China Mater*, 2018, 61: 1019–1020
- Lu K, Lu L, Suresh S. Strengthening materials by engineering coherent internal boundaries at the nanoscale. *Science*, 2009, 324: 349–352
- Shute CJ, Myers BD, Xie S, *et al.* Detwinning, damage and crack initiation during cyclic loading of Cu samples containing aligned nanotwins. *Acta Mater*, 2011, 59: 4569–4577
- Li LL, Zhang ZJ, Zhang P, *et al.* Controllable fatigue cracking mechanisms of copper bicrystals with a coherent twin boundary. *Nat Commun*, 2014, 5: 3536
- Pan Q, Zhou H, Lu Q, *et al.* History-independent cyclic response of nanotwinned metals. *Nature*, 2017, 551: 214–217
- Li X, Wei Y, Lu L, *et al.* Dislocation nucleation governed softening and maximum strength in nano-twinned metals. *Nature*, 2010, 464: 877–880

- 10 Frøseth AG, Derlet PM, Van Swygenhoven H. Grown-in twin boundaries affecting deformation mechanisms in nc-metals. *Appl Phys Lett*, 2004, 85: 5863–5865
- 11 Sun S, Li D, Yang C, *et al.* Direct atomic-scale observation of ultrasmall Ag nanowires that exhibit fcc, bcc, and hcp structures under bending. *Phys Rev Lett*, 2022, 128: 015701
- 12 Zheng GP, Wang YM, Li M. Atomistic simulation studies on deformation mechanism of nanocrystalline cobalt. *Acta Mater*, 2005, 53: 3893–3901
- 13 Frøseth A, Van Swygenhoven H, Derlet PM. The influence of twins on the mechanical properties of nc-Al. *Acta Mater*, 2004, 52: 2259–2268
- 14 Zhu T, Li J, Samanta A, *et al.* Interfacial plasticity governs strain rate sensitivity and ductility in nanostructured metals. *Proc Natl Acad Sci USA*, 2007, 104: 3031–3036
- 15 Wei Y. The kinetics and energetics of dislocation mediated de-twinning in nano-twinned face-centered cubic metals. *Mater Sci Eng-A*, 2011, 528: 1558–1566
- 16 Shabib I, Miller RE. Deformation characteristics and stress-strain response of nanotwinned copper *via* molecular dynamics simulation. *Acta Mater*, 2009, 57: 4364–4373
- 17 Fu L, Yang C, Lu Y, *et al.* *In situ* atomistic mechanisms of detwinning in nanocrystalline AuAg alloy. *Sci China Mater*, 2022, 65: 820–826
- 18 Yamakov V. Deformation twinning in nanocrystalline Al by molecular-dynamics simulation. *Acta Mater*, 2002, 50: 5005–5020
- 19 Li N, Wang J, Huang JY, *et al.* Influence of slip transmission on the migration of incoherent twin boundaries in epitaxial nanotwinned Cu. *Scripta Mater*, 2011, 64: 149–152
- 20 Wang J, Li N, Anderoglu O, *et al.* Detwinning mechanisms for growth twins in face-centered cubic metals. *Acta Mater*, 2010, 58: 2262–2270
- 21 Wu XL, Liao XZ, Srinivasan SG, *et al.* New deformation twinning mechanism generates zero macroscopic strain in nanocrystalline metals. *Phys Rev Lett*, 2008, 100: 095701
- 22 Liang Y, Yang X, Gong M, *et al.* Slip transmission for dislocations across incoherent twin boundary. *Scripta Mater*, 2019, 166: 39–43
- 23 Guo Y, Wang Z, Zhang B, *et al.* Twin thickness and dislocation interactions affect the incoherent-twin boundary phase in face-centered cubic metals. *Cell Rep Phys Sci*, 2022, 3: 100736
- 24 Olmsted DL, Foiles SM, Holm EA. Survey of computed grain boundary properties in face-centered cubic metals: I. Grain boundary energy. *Acta Mater*, 2009, 57: 3694–3703
- 25 Yang CC, Rollett AD, Mullins WW. Measuring relative grain boundary energies and mobilities in an aluminum foil from triple junction geometry. *Scripta Mater*, 2001, 44: 2735–2740
- 26 Saylor DM, El Dasher BS, Rollett AD, *et al.* Distribution of grain boundaries in aluminum as a function of five macroscopic parameters. *Acta Mater*, 2004, 52: 3649–3655
- 27 Frolov T, Olmsted DL, Asta M, *et al.* Structural phase transformations in metallic grain boundaries. *Nat Commun*, 2013, 4: 1899
- 28 Zhu Q, Samanta A, Li B, *et al.* Predicting phase behavior of grain boundaries with evolutionary search and machine learning. *Nat Commun*, 2018, 9: 467
- 29 Carrion F, Kalonji G, Yip S. Evidence for grain boundary phase transition in a 2D bicrystal. *Scripta Metall*, 1983, 17: 915–918
- 30 Frolov T, Setyawan W, Kurtz RJ, *et al.* Grain boundary phases in bcc metals. *Nanoscale*, 2018, 10: 8253–8268
- 31 Chua ALS, Benedek NA, Chen L, *et al.* A genetic algorithm for predicting the structures of interfaces in multicomponent systems. *Nat Mater*, 2010, 9: 418–422
- 32 Meiners T, Frolov T, Rudd RE, *et al.* Observations of grain-boundary phase transformations in an elemental metal. *Nature*, 2020, 579: 375–378
- 33 Sheng HW, Kramer MJ, Cadien A, *et al.* Highly optimized embedded-atom-method potentials for fourteen fcc metals. *Phys Rev B*, 2011, 83: 134118
- 34 Hirel P. Atomsk: A tool for manipulating and converting atomic data files. *Comput Phys Commun*, 2015, 197: 212–219
- 35 Plimpton S. Fast parallel algorithms for short-range molecular dynamics. *J Comput Phys*, 1995, 117: 1–19
- 36 Stukowski A. Visualization and analysis of atomistic simulation data with OVITO—The open visualization tool. *Model Simul Mater Sci Eng*, 2010, 18: 015012
- 37 Wang J, Misra A, Hirth JP. Shear response of $\Sigma 3$ {112} twin boundaries in face-centered-cubic metals. *Phys Rev B*, 2011, 83: 064106
- 38 Wang J, Anderoglu O, Hirth JP, *et al.* Dislocation structures of $\Sigma 3$ {112} twin boundaries in face centered cubic metals. *Appl Phys Lett*, 2009, 95: 021908
- 39 Wang C, Du K, Song K, *et al.* Size-dependent grain-boundary structure with improved conductive and mechanical stabilities in sub-10-nm gold crystals. *Phys Rev Lett*, 2018, 120: 186102
- 40 Wang L, Zhang Y, Zeng Z, *et al.* Tracking the sliding of grain boundaries at the atomic scale. *Science*, 2022, 375: 1261–1265
- 41 Pan Q, Lu L. Dislocation characterization in fatigued Cu with nanoscale twins. *Sci China Mater*, 2015, 58: 915–920

Acknowledgements This work was supported by the National Key R&D Program of China (2021YFA1200201), Beijing Outstanding Young Scientists Projects (BJJWZYJH01201910005018), the National Natural Science Foundation of China (12174014 and 12372106), and the Fundamental Research Funds for the Central Universities (YMF-22-L-808).

Author contributions Wang Z conducted the molecular statics simulations; Guo Y, Ma Y and Yang C conducted the data statistics; Han X, Wang L and Zhai Y designed the project and guided the research; Wang Z, Yan X and Wang L wrote the manuscript. All authors have discussed and approved the results and conclusions.

Conflict of interest The authors declare that they have no conflict of interest.

Supplementary information Supporting data are available in the online version of the paper.



Zhanxin Wang is a PhD candidate at Beijing Key Laboratory and the Institute of Microstructure and Properties of Advanced Materials, Beijing University of Technology. His research focuses on the atomic-scale *in-situ* mechanics of FCC metallic materials based on *in-situ* transmission electron microscopy and molecular dynamics simulations.



Yadi Zhai is an assistant professor at Beijing University of Technology. He originally developed the atomic-level *in-situ* dynamic characterization method of the mechanical behavior of materials, and increased the spatial resolution of the *in-situ* characterization technology, achieving an order of magnitude improvement. His research focuses on the physical and chemical properties of materials, the mechanical behavior of materials from micro-nano to atomic resolution.



Xin Yan is currently an associate professor at the school of mechanical engineering and automation, Beihang University. She received her BS degree in mechanical engineering from Beijing Institute of Technology, MSc degree from the University of Saskatchewan (Canada) and PhD degree from the University of Houston (US). Her research is centered on the mechanics of solids using multiscale modeling approaches, atomistic simulation of plastic deformation of metal and metallic glasses.



Lihua Wang is a professor at Beijing University of Technology. He has been engaged in “*in-situ* experimental research on the mechanical behavior of materials at the atomic scale”. For the first time, the atomic-scale *in-situ* observation of grain boundary deformation mechanisms in metal polycrystals has been realized.

面心立方金属中非共格孪晶界原子结构的孪晶厚度效应研究

王占鑫¹, 郭谊忠¹, 马琰¹, 杨成鹏¹, 翟亚迪^{1*}, 燕鑫^{2*}, 王立华^{1*}, 韩晓东¹

摘要 非共格孪晶界(ITB)能显著影响金属力学性能, 受到了研究者极大关注. 理论模型预测ITB是由系列偏位错组成, ITB两侧的晶面没有沿[111]方向的相对位移. 本文利用分子静力学模拟研究了Ag, Cu, Ni和Al中ITB的结构, 发现ITB的结构具有显著的尺寸效应. 对于较薄的ITB, 界面两侧的晶面处于同一水平面, 没有沿[111]方向的相对位移, 与理论模型结果一致. 而对于较厚的ITB, 界面两侧的晶面有明显的[111]方向的相对位移, 且相对位移随着ITB厚度的增加而增加. 此外, 研究揭示出ITB两侧晶面沿[111]方向的位移与金属的层错能直接相关. 该研究表明ITB的结构并不唯一, 不同的厚度、层错能对应不同的ITB结构. 本研究为理解孪晶厚度和层错能对金属力学性能的影响提供了新见解.